Intermolecular Interactions in the Crystal Chemistry of *N,N′*-Diphenylisophthalamide, Pyridine-2,6-dicarboxylic Acid Bisphenylamide, and Related Compounds

J. F. Malone,* C. M. Murray, and G. M. Dolan

School of Chemistry, The Queen's University of Belfast, Belfast, BT9 5AG, UK

R. Docherty and A. J. Lavery

Zeneca Specialties, Research Centre, P.O. Box 42, Hexagon House, Blackley, Manchester M9 8ZS, UK

Received May 9, 1997[⊗]

The synthesis, characterization, and crystal chemistry of *N,N′*-diphenylisophthalamide (**1**) and pyridine-2,6-dicarboxylic acid bisphenylamide (**2**) are described. Through a combination of single-crystal X-ray diffraction and molecular orbital and crystal packing calculations, the important intermolecular interactions have been determined. The structures have been compared with the closely related structures, *N,N′*-bis(3-hydroxyphenyl)isophthalamide (**3**) and *N,N′*-dimethyl-*N,N′*-diphenylisophthalamide (**4**). Crystalline **1** and **2** are isostructural, but there are subtle differences in the conformations and packing as a consequence of intramolecular hydrogen bonding in **2**. This reduces the deviation from planarity in the molecular conformation of **2** and consequently lengthens the intermolecular hydrogen bonding distances. This is reflected in the lattice energies of **1** and **2** (−40.9 and −38.7 kcal/mol, respectively) and in the stacking energies of these compounds. For the compounds that do not contain an N atom in the central ring the progression **3**, **1**, **4** represents a reduction in the hydrogen-bonding options, reflected in the respective lattice energies: −51.3, −40.9, and −33.3 kcal/mol. The difference between **3** and **1** is in excellent agreement with predictions based on group contributions in structure **3**. In **4** there are no hydrogen bonding options and so C−H···O interactions play a much more important role.

Introduction

An organic crystal is an example of a near-perfect supramolecular assembly. The result of a crystallization process is the gathering together of millions of molecules into a unique ordered arrangement. This gathering is reproducible under the same crystallization conditions. Polymorphism, the adoption of different solid-state arrangements by the same molecular system, is due to the recognition of a slightly different subtle balance of these interactions. The solid-state arrangements, adopted by molecular materials, are the result of an "intermolecular synthesis"[1] which is a sum of the individual atom−atom interactions. Solid-state structures are the result of molecular recognition on a grand scale.[1−6]

The design of synthetic receptors within supramolecular assemblies is a fast growing area of chemistry, the aim being to use intermolecular forces to encapsulate small organic guest molecules to function as sensors or in catalysis performing specific chemical reactions.[7,8] Structures similar to that reported here have been shown to act as models for the active site of ribonuclease A.[9]

Crucial to the design of supramolecular assemblies is the understanding of the relative importance of different interaction types. Graph theory has been used to describe different hydrogen-bonding patterns found in molecular materials.[3] More recently, work has focused on the role of weaker intermolecular interactions in solid-state structures.[10,11]

In this paper we report the synthesis, characterization, and crystal chemistry of *N,N′*-diphenylisophthalamide (**1**) and pyridine-2,6-dicarboxylic acid bisphenylamide (**2**) (Figure 1). Through a combination of single-crystal X-ray diffraction, molecular orbital, and crystal packing calculations the important intermolecular interactions have been determined. The crystal chemistry of **1** and **2** is compared with the closely related structures *N,N′*-bis(3-hydroxyphenyl)isophthalamide[12] (**3**) and *N,N′*-dimethyl-*N,N′*-diphenylisophthalamide[13] (**4**).

[⊗] Abstract published in *Advance ACS Abstracts,* October 15, 1997.

(1) Desiraju, G. R. *Angew. Chem., Int. Ed. Engl.* **1995**, *34*, 2311.
(2) Dunitz, J. D. *Pure Appl. Chem.* **1991**, *63*, 177.
(3) Etter, M. C. *J. Phys. Chem.* **1991**, *95*, 4601.
(4) Aakeröy, C. B.; Seddon, K. R. *Chem. Soc. Rev.* **1993**, *22*, 397.
(5) MacDonald, J. C.; Whitesides, G. M. *Chem. Rev. (Washington, D.C.)* **1994**, *94*, 2383.
(6) Fan, E.; Vicent, C.; Geib, S. J.; Hamilton, A. D. *Chem. Mater.* **1994**, *6*, 1113.
(7) Webb, T. H.; Wilcox, C. S. *Chem. Soc. Rev.* **1993**, 383.
(8) Lehn, J. M. *Angew. Chem., Int. Ed. Engl.* **1990**, *29*, 1304.
(9) Kato, T.; Takeuchi, T.; Karube, I. *J. Chem. Soc., Chem. Commun.* **1996**, 953.
(10) Desiraju, G. R. *Acc. Chem. Res* **1991**, *24*, 290.
(11) Pedireddi, V. R.; Jones, W.; Chorlton, A. P.; Docherty, R. *J. Chem. Soc., Chem. Commun.* **1996**, 987. Pedireddi, V. R.; Jones, W.; Chorlton, A. P.; Docherty, R. *J. Chem. Soc., Chem. Commun.* **1996**, 997.
(12) Malone, J. F.; Murray, C. M.; Nieuwenhuyzen, M.; Stewart, G.; Docherty, R.; Lavery, A. J. *Chem. Mater.* **1997,** *7*, 334.
(13) Yamaguchi, K.; Matsumura, G.; Kgechika, H.; Azumaya, I.; Ito, Y.; Itai, A.; Shudo, K. *J. Am. Chem. Soc.* **1991,** 5474.

S0897-4756(97)00350-5 CCC: $14.00

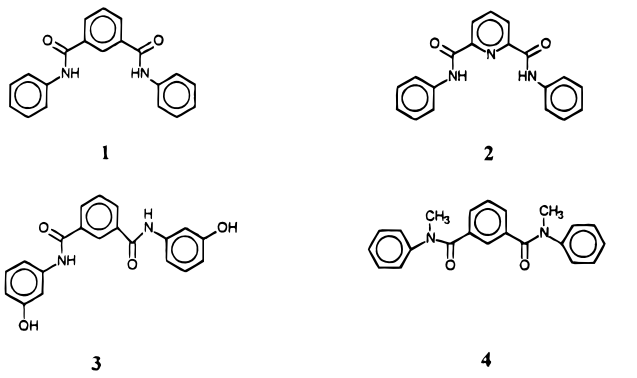

Figure 1.

The structures **1**−**4** have a varying number of potential hydrogen-bonding sites, decreasing in the order **3**, **2**, **1**, **4**. In **2** there is a potential intramolecular hydrogen bond in competition with intermolecular bonding interactions. Understanding the relative importance of these interaction types forms the basis for an ongoing study of host−guest interactions in the solid state. This uses **1**, **2**, and **3** as host structures to encapsulate smaller organic systems, such as urea and barbital, as guests[12] in a manner similar to that previously reported.[6]

Experimental Section

General Methods of Preparation. *N,N′-Diphenylisophthalamide (1).* The product **1** was formed by a condensation reaction between isophthaloyl dichloride and aniline in 92.4% yield. Isophthaloyl dichloride (1.003 g, 0.005 mol) was dissolved in acetonitrile (50 mL), and this was added to an excess of aniline (0.919 g, 0.01 mol) also dissolved in acetonitrile. The mixture was refluxed at 70−80° over a water bath for 1 h to ensure complete reaction. The precipitate was then filtered with suction and dried. Single crystals were obtained as colorless blocks from dry DMF as a result of slow evaporation over 4 months. Found: C, 75.48; H, 5.00; N, 8.75. $C_{20}H_{16}N_2O_2$ requires C, 75.94; H, 5.06; N, 8.86%. δ_H (500 MHz, $(CD_3)_2SO$) 7.10−8.52 (14H, m, Ar), 10.39 (2H, s, NH); m/z = 316 (EI); mp 287 °C.

Pyridine-2,6-dicarboxylic Acid Bisphenylamide (2). The product **2** was formed by a condensation reaction between 2,6-pyridine dicarbonyldichloride and aniline in 70.4% yield. The same procedure as above was followed using 1.005 g (0.005 mol) of 2,6-pyridine dicarbonyldichloride and 1.12 g (0.012 mol) of aniline. The single crystals were obtained as colorless blocks from a methanol solution by slow evaporation over 4 months. Found: C, 71.63; H, 4.68; N, 13.18. $C_{19}H_{15}N_3O_2$ requires C, 71.92; H, 4.73; N, 13.25%. δ_H (500 MHz, $(CD_3)_2SO$) 7.17−8.41 (13H, m, Ar), 11.02 (2H, s, NH); m/z = 317 (EI); mp 274 °C.

Crystal Structure Determination. *Data Collection and Processing.* The crystals selected for analysis were 0.44 × 0.38 × 0.26 mm (**1**) and 0.26 × 0.26 × 0.22 mm (**2**) in size. Data were collected on a Siemens P4 four-circle diffractometer with Mo Kα (graphite monochromated, λ = 0.7107 Å) radiation at 293 K. Crystal stability was checked every 100 reflections and showed no significant variation (±1%). Cell parameters were determined from 38 accurately centered reflections in the 2θ range 20−25° for **1** and from 35 reflections in the 2θ range 14−23° for **2**. 2996 reflections were collected over the range $5 < 2\theta < 50°$ for $0 < h < 14$, $0 < k < 14$, and $-27 < l < 26$ for **1** and 2124 reflections were collected over the range $5 < 2\theta < 45°$ for $0 < h < 12$, $0 < k < 12$, and $-23 < l < 22$ for **2**. In each case Lorentz and polarization corrections were applied. Of the 2916 independent reflections collected 1923 with $F > 4\sigma(F)$ were used in the final refinement of **1** and of the 2123 independent reflections collected 1479 were used in the final refinement of **2**. Crystal data are listed in Table 1. The crystals of **1** were poor in quality, yielding poor diffraction data.

Table 1. Crystallographic Data

	1	**2**
formula	$C_{20}H_{16}N_2O_2$	$C_{19}H_{15}N_3O_2$
M	316.35	317.34
crystal size (mm)	0.44 × 0.38 × 0.26	0.26 × 0.26 × 0.22
crystal system	monoclinic	monoclinic
space group	*Cc*	*Cc*
Z	8	8
a (Å)	11.827(2)	12.024(2)
b (Å)	11.828(2)	12.021(2)
c (Å)	23.211(2)	21.932(3)
β (deg)	102.89(1)	103.17(1)
U (Å^3)	3165.2(8)	3086.7(8)
range *h*	0−14	0−12
range *k*	0−14	0−12
range *l*	−27 to 26	−23 to 22
D_c (g cm^{-3})	1.328	1.366
F(000)	1328	1328
ω scans: θ range (deg)	2.47−25	2.43−22.49
total reflections	2916	2123
reflections in final cycles	1923	1479
parameters refined	433	433
residual density (e Å^{-3})	1.40	0.16
goodness of fit	1.05	0.99
*wR*2 (all data)	0.393	0.0885
*R*1 ($F > 4\sigma(F)$)	0.1191	0.0444
temp (K)	293	293

Structure Solution and Refinement. The structures were determined by direct methods and non-hydrogen atoms were refined with allowance for anisotropic vibrations. All hydrogen atoms were located in a difference Fourier map for **2**, but were not located for **1**. In the refinement all hydrogens for both compounds were included using the riding model with temperature factors, U_{iso}, fixed at 1.2 U(eq) for the attached atom. The XSCANS,[14] SHELXTL PC,[15] and SHELXL-93[16] software packages were used for data collection, reduction, and structure solution and refinement. The final R factor was R_1 = 0.1191 for 1923 data (**1**) and R_1 = 0.0444 for 1479 data (**2**) with $F > 4\sigma|F_o|$. Because of the high R_1 value for **1**, resulting from the poor crystals and consequent low-quality diffraction data and high estimated standard deviations for all parameters, no specific claims are made, *in isolation*, for this structure. The conclusions are based on the accurate determination of structure **2**, together with the fact that the two compounds are isostructural.

Results and Discussion

Molecular Structures. The crystal structures of **1** and **2** were determined as described in the Experimental Section. The crystallographic data are summarized in Table 1, and atomic coordinates are given in Tables 2 and 3. The compounds are isomorphous and isostructural, each containing two independent, but conformationally equivalent, molecules in the asymmetric unit. These two molecules are related by an approximate, noncrystallographic center of symmetry at 0, $^1/_8$, 0. As this point does not lie on the glide plane at y = 0, and cannot be moved to this plane by change of origin, the space group is correctly assigned as *Cc* rather than the higher symmetry *C*2/*c* (which would require only one molecule per asymmetric unit). The potential conformations for the molecules (i.e., syn−syn, syn−anti, and anti−anti) are shown in Figure 2. The molecular conformation of one molecule of **1** is shown in Figure 3 and that of **2** in Figure 4, both being syn−syn. Each amido moiety is twisted relative to the central aromatic

(14) XSCANS, Siemens Analytical X-ray Instruments, Inc., Madison, WI, 1994.
(15) Sheldrick, G. M. SHELXTL PC, Siemens Analytical X-ray Instruments, Inc., Madison, WI, 1990.
(16) Sheldrick, G. M. SHELXL-93, University of Göttingen, 1993.

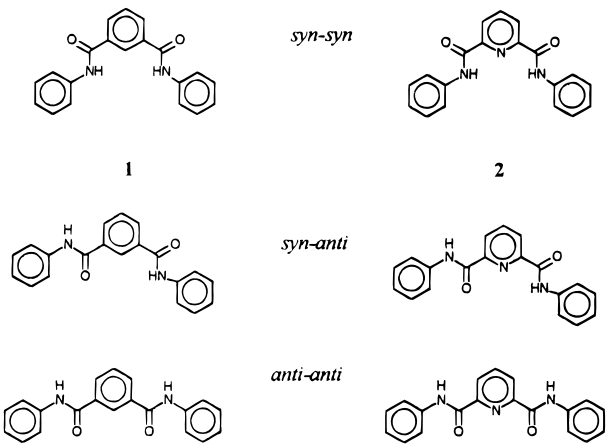

Figure 2. Possible conformations of **1** and **2**. The crystal structures show the conformation to be syn−syn for both compounds.

Table 2. Atomic Fractional Coordinates and ESDs [×10⁴] for 1

atom	*x*	*y*	*z*
C(1A)	401(15)	−2675(16)	−1301(8)
C(2A)	189(19)	−3642(19)	−1644(9)
C(3A)	764(16)	−3925(13)	−2030(8)
C(4A)	1737(15)	−3184(17)	−2060(7)
C(5A)	2015(16)	−2306(13)	−1699(6)
C(6A)	1354(13)	−2043(11)	−1324(6)
C(7A)	2631(11)	−589(10)	−743(6)
C(8A)	2590(12)	431(12)	−321(6)
C(9A)	3412(15)	1232(15)	−318(7)
C(10A)	3466(15)	2109(15)	20(8)
C(11A)	2604(12)	2292(11)	369(7)
C(12A)	1801(12)	1482(11)	370(7)
C(13A)	1799(11)	481(11)	19(6)
C(14A)	1034(10)	1665(10)	749(6)
C(15A)	−138(13)	1421(13)	1780(7)
C(16A)	−1013(17)	1361(12)	2125(7)
C(17A)	−1747(18)	572(17)	2084(9)
C(18A)	−1724(16)	−295(19)	1660(10)
C(19A)	−893(16)	−224(15)	1301(7)
C(20A)	−156(10)	645(12)	1353(5)
N(1A)	1599(10)	−1058(9)	−950(5)
N(2A)	641(9)	730(9)	968(5)
O(1A)	3549(9)	−953(8)	−834(5)
O(2A)	722(9)	2653(8)	863(5)
C(1B)	−372(15)	5216(17)	1327(7)
C(2B)	−96(17)	6164(18)	1679(8)
C(3B)	−941(18)	6386(13)	2068(8)
C(4B)	−1749(15)	5702(15)	2117(8)
C(5B)	−1943(15)	4757(15)	1768(6)
C(6B)	−1251(14)	4508(11)	1357(6)
C(7B)	−2572(11)	3068(10)	748(5)
C(8B)	−2577(12)	2120(10)	373(6)
C(9B)	−3411(11)	1295(11)	358(7)
C(10B)	−3397(14)	279(12)	17(8)
C(11B)	−2617(11)	161(14)	−323(6)
C(12B)	−1805(13)	1010(12)	−332(6)
C(13B)	−1742(12)	1934(10)	21(5)
C(14B)	−956(11)	814(10)	−731(5)
C(15B)	289(14)	1018(12)	−1754(7)
C(16B)	940(16)	1091(16)	−2113(8)
C(17B)	1756(15)	2012(17)	−2034(7)
C(18B)	1723(17)	2852(15)	−1635(8)
C(19B)	962(21)	2755(15)	−1277(8)
C(20B)	223(14)	1807(13)	−1328(7)
N(1B)	−1543(9)	3549(9)	979(5)
N(2B)	−568(10)	1755(9)	−943(5)
O(1B)	−3511(8)	3424(8)	849(4)
O(2B)	−666(9)	−150(8)	−838(5)

ring. The values of the twists for molecules **1**−**4** are given in Table 4. In **1** and **2** the mean interplanar angles are 31° and 24°, while in **3** they are dependent on the conformation (i.e., syn or anti). In **2** the twist

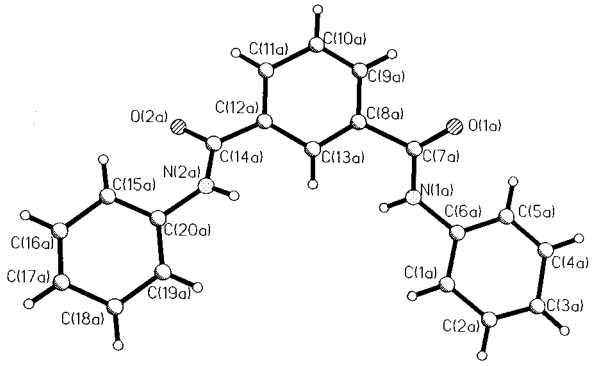

Figure 3. Crystallographic projection of one molecule of compound **1**.

Table 3. Atomic Fractional Coordinates and ESDs [×10⁴] for 2

atom	*x*	*y*	*z*
C(1A)	418(10)	−2581(9)	−1209(5)
C(2A)	93(10)	−3470(9)	−1596(5)
C(3A)	750(14)	−3840(11)	−2000(7)
C(4A)	1767(13)	−3242(11)	−2009(7)
C(5A)	2076(9)	−2320(9)	−1623(5)
C(6A)	1418(8)	−2007(7)	−1210(5)
C(7A)	2725(7)	−584(6)	−633(4)
C(8A)	2707(9)	472(8)	−259(5)
C(9A)	3575(8)	1207(8)	−266(5)
C(10A)	3555(9)	2225(9)	74(6)
C(11A)	2680(9)	2402(8)	376(5)
C(12A)	1933(8)	1530(9)	376(5)
N(13A)	1920(6)	586(6)	73(4)
C(14A)	1033(7)	1702(6)	754(4)
C(15A)	−266(9)	1460(8)	1774(5)
C(16A)	−1006(12)	1303(11)	2151(6)
C(17A)	−1645(12)	374(10)	2109(7)
C(18A)	−1554(11)	−413(10)	1688(6)
C(19A)	−798(9)	−298(9)	1308(5)
C(20A)	−143(8)	659(8)	1332(5)
N(1A)	1703(5)	−1090(5)	−805(3)
N(2A)	596(5)	761(5)	927(3)
O(1A)	3614(4)	−903(4)	−764(3)
O(2A)	777(5)	2644(4)	899(3)
C(1B)	−353(10)	5077(9)	1335(5)
C(2B)	−82(10)	6038(9)	1698(6)
C(3B)	−753(12)	6355(10)	2080(6)
C(4B)	−1678(13)	5756(11)	2122(6)
C(5B)	−1984(8)	4830(8)	1750(5)
C(6B)	−1332(8)	4487(7)	1346(4)
C(7B)	−2613(6)	3032(6)	765(4)
C(8B)	−2632(9)	2021(9)	381(5)
C(9B)	−3442(9)	1207(7)	384(5)
C(10B)	−3438(9)	252(8)	63(6)
C(11B)	−2611(8)	119(8)	−270(5)
C(12B)	−1789(8)	922(7)	−258(4)
N(13B)	−1788(6)	1881(6)	77(4)
C(14B)	−928(6)	764(6)	−635(4)
C(15B)	375(9)	990(9)	−1641(5)
C(16B)	1130(11)	1136(12)	−2040(6)
C(17B)	1784(12)	2116(12)	−2000(7)
C(18B)	1604(9)	2988(9)	−1593(5)
C(19B)	872(10)	2810(10)	−1206(6)
C(20B)	279(8)	1832(7)	−1224(5)
N(1B)	−1599(5)	3553(5)	948(3)
N(2B)	−473(5)	1722(5)	−808(3)
O(1B)	−3511(5)	3373(4)	894(3)
O(2B)	−668(5)	−175(4)	−765(3)

angles are slightly less due to the formation of intramolecular NH···N(pyridine) hydrogen bonds (in the range 2.33−2.38 Å). The presence of this hydrogen-bonding interaction in **2** is also indicated from the NMR spectra in $(CD_3)_2SO$ solution, by a downfield shift of 0.63 ppm for the NH signal in **2** compared with that in **1** (δ 11.02 and 10.39 ppm, respectively).

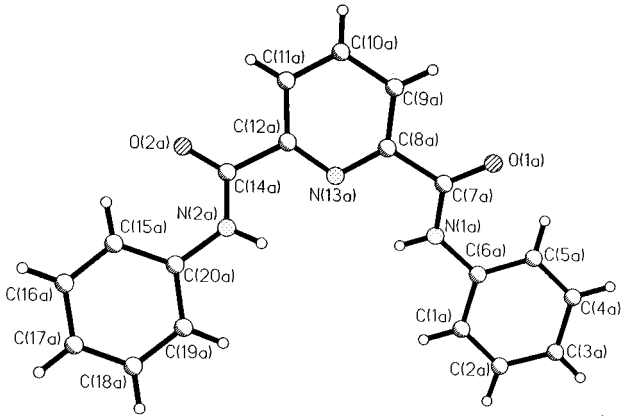

Figure 4. Crystallographic projection of one molecule of compound **2**.

Table 4. Twist Angles of the Amido Units Relative to the Central Ring Plane

compound	motif type	mean twist (deg)
1	syn−syn	31
2	syn−syn	24
3	syn−anti	26 (anti), 39 (syn)
4	anti−anti	50

Table 5. Calculated Heats of Formation of Conformations (As Shown in Figure 2)

	$-H_f$ (kcal/mol)			
motif	**1**	**2**	**3**[a]	**4**
syn−syn	17.37	28.41	−69.96	57.69[c]
syn−anti	18.12	32.42	−72.25	37.18
anti−anti	20.41	41.10[b]	−67.13	38.83

[a] Taken from ref 12. [b] 1 SCF calculation based on set anti−anti geometry. If optimized, the structure relaxed to syn−anti. [c] 1 SCF calculation based on set syn−syn geometry. Value is high due to methyl group repulsions.

Calculations were carried out to investigate the conformational preference of structures **1**, **2**, **3**, and **4**. Using MOPAC (v. 6.0)[17] the structures of the syn−syn, syn−anti, anti−anti conformations (Figure 2) were optimized at the AM1 level.[18] The default minimization criteria were employed along with the molecular mechanics correction needed to reproduce the structural features of the amide linkage. The heats of formation for the various conformers are given in Table 5.

The preference for the syn−syn conformation (by around 0.75 kcal/mol for **1** and 4.0 kcal/mol for **2**) agrees with that observed in the crystal structure. The heat of formation for the anti−anti conformation is estimated from single-point energy calculations as on optimization the molecule twisted into the syn−anti conformation. Structure **2** is much more stable in the syn−syn motif. The difference in the energy of the syn−syn and syn−anti conformations (ca. 4.0 kcal/mol for **2**) is consistent with the energy required to break an intramolecular hydrogen bond. The anti−anti conformer for **2** is 12.7 kcal/mol less stable than the syn−syn conformation as this involves breaking two intramolecular hydrogen bonds. As discussed elsewhere[12] structure **3** prefers the syn−anti conformation. Calculations suggest that structure **4** should adopt the syn−anti conformation in preference to the anti−anti conformation by 1.6 kcal/mol but the anti−anti arrangement is that observed in the solid-state structure. This would imply that in **4** the intermolecular interactions formed in the solid override the intramolecular interactions.

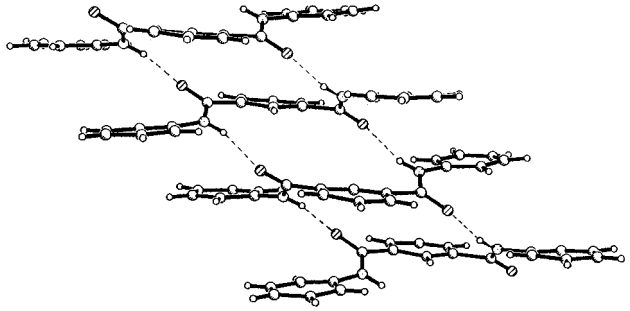

Figure 5. Intermolecular interactions between C═O and N−H groups (illustrated here for **1**).

Crystal Packing and Interatomic Contacts. Compounds **1** and **2** are isostructural. They adopt space group *Cc* with two molecules in the asymmetric unit. Both molecules in the asymmetric unit adopt a syn−syn arrangement. Each molecule is involved in four hydrogen bonds involving the C═O and N−H units. The torsion angles of the H−N−C═O units are approximately 180° and a C═O unit of one molecule interacts with an N−H unit of a molecule above and below. This motif is shown in Figure 5.

The most interesting difference between **1** and **2** is the subtle changes in the hydrogen-bonding contacts. These important interactions are given in Table 6. The intermolecular N−H···O contacts in **2** are longer than in **1**. This is a result of the intramolecular N−H··· N(pyridine) hydrogen bonding in **2**, which reduces the twist between the pyridine and amide planes and consequently increases the intermolecular hydrogen-bond distances and weakens the intermolecular interactions. Etter's rules[3] predict that the formation of an intramolecular hydrogen bond to form pseudo 5- or 6-membered rings takes precedence over any other form of hydrogen bonding.

The benzene analogue **1** also involves the formation of weak intermolecular C−H···O interactions between C13−H and the carbonyl oxygens. These are supporting interactions to the N−H···O hydrogen bonds and occur with both the molecule above and below. The geometric details of these weaker interactions are given in Table 7.

The cavity formed within molecules **1** and **2** is slightly different in geometry, but the packing arrangement of the crystal is the same. Each structure packs so that the central ring of one molecule fits into the cavity of another, as shown in Figure 6. In **1** the C13···H10′ distance is 4.68 Å, and in **2** the N13···H10′ distance is 4.78 Å. It is perhaps unexpected that the distance should be longer for the pyridine structure, but this can be explained as a consequence of the intramolecular hydrogen bonding which causes the cavity in **2** to be tighter.

Both crystal structures **1** and **2** can be described as stacks of molecules linked by N−H···O hydrogen bonds. In each molecule each N−H group is used to donate a hydrogen bond and each C═O group accepts a hydrogen bond. For an individual molecule these interactions

(17) MOPAC (v. 6.0) Quantum Chemistry Program Exchange Program No. 455. Creative Arts Building 181, Indiana University, Bloomington, IN 47405.

(18) Dewar, M. J. S.; Zoebisch, E. G; Healy E. F.; Stewart, J. J. P. *J. Am. Chem. Soc.* **1985**, *107*, 3902.

Table 6. Geometric Details of the Hydrogen Bonds in 1 and 2

structure	atoms involved	mean distance/Å: donor···acceptor	mean distance/Å: hydrogen···acceptor	donor−H···acceptor angle, deg
1	N1A(/B)-H···O2B(/A)	2.95	2.11	164.0
	N2A(/B)-H···O1B(/A)[a]	2.94	2.10	163.9
2	N2A(/B)-H···O2B(/A)	3.08	2.29	152.5
	N1A(/B)-H···O1B(/A)[a]	3.07	2.29	150.8
intramolecular	N1-H···N13	2.75	2.36	108.5
	N2-H···N13	2.75	2.35	108.8

[a] $^1/_2 + x, -^1/_2 + y, z/-^1/_2 + x, ^1/_2 + y, z$.

Table 7. Weak Intermolecular Interactions in 1−4

structure	atoms involved	mean distance/Å: donor···acceptor	mean distance/Å: hydrogen···acceptor	donor−H···acceptor angle, deg
1	C13A-H···O1B[b]	3.18	2.56	124.4
	C13A-H···O2B	3.23	2.69	117.5
	C13B-H···O2A	3.24	2.60	126.5
	C13B-H···O1A[c]	3.26	2.72	117.5
2	none			
3	C13-H13···O1[d]	2.57	3.14	118.2
	C11-H11···O4[e]	2.67	3.50	145.7
	C15-H15···O3[f]	2.61	3.30	129.8
4	C4-H···O2	2.62	3.42	133.4
	C19-H···O2	2.29	3.26	162.1
	C18-H···O1	2.58	3.46	132.9
	C9-H···C18	2.83	3.65	137.9
	C21-H···C16	2.84	3.70	161.5

[b] $^1/_2 + x, -^1/_2 + y, z$. [c] $-^1/_2 + x, ^1/_2 + y, z$. [d] $-x, 1 - y, 2 - z$. [e] $1 - x, 2 - y, 1 - z$. [f] $-x, 2 - y, 1 - z$.

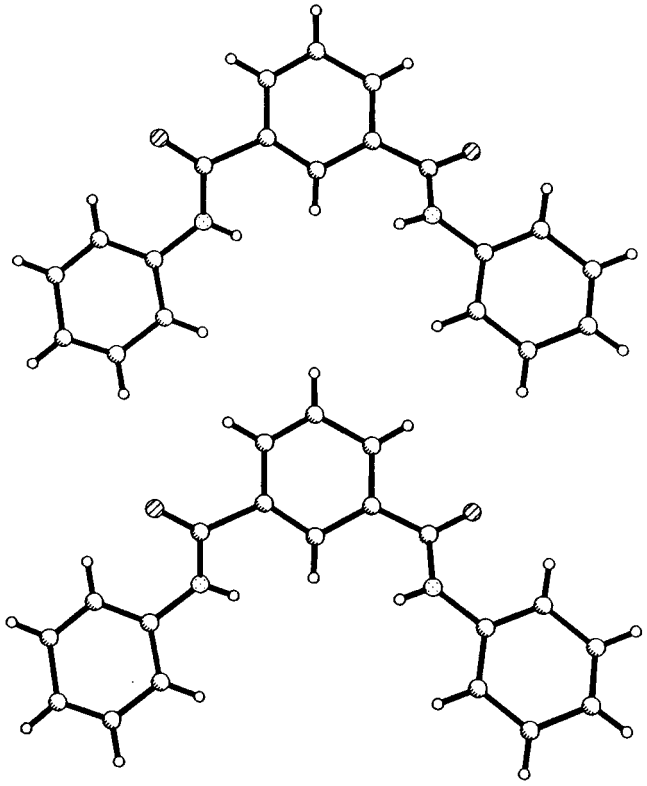

Figure 6. Fitting of adjacent molecules (illustrated here for **1**).

involve the molecules above and below in the stack which follows approximately the direction of the unit cell *abc* body diagonal. Each stack fits into the next (approximately along the $-a,b$ diagonal) by means of the cavity fitting described earlier. In addition $\pi-\pi$ stacking is evident, with a single molecule interacting with half a molecule above and below, as shown in Figure 7. The separation of the layers is 3.54 Å for **1** and 3.48 Å for **2**. The values were calculated as the

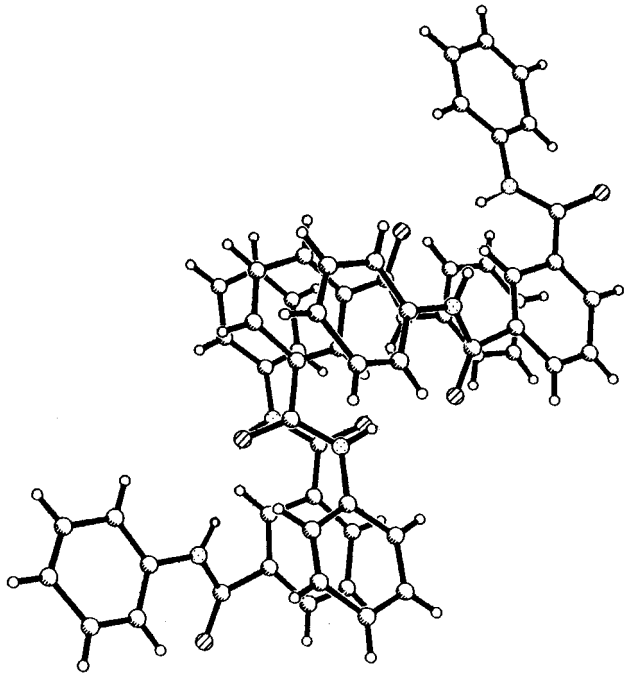

Figure 7. $\pi-\pi$ stacking in **1**.

average perpendicular distance from the plane of the half molecule above. These stacks are connected in a "herringbone" style through long-range T-bonds between H4 and H17 and the two pendent phenyl rings.

As described earlier[12] the solid-state structure of **3** is dominated by hydrogen bonding motifs between the syn and anti conformers. Each unit recognizes itself and the syn−syn and anti−anti hydrogen bond pairings are supplemented by weaker C−H···O contacts.

Molecule **4** adopts the anti−anti formation. The syn−syn conformation is not possible due to the steric hindrance between the $-CH_3$ groups. This is reflected by the high heat of formation for the syn−syn confor-

Table 8. Lattice Energies[a]

structure	total lattice energy (kcal/mol)
1	−40.89
2	−38.75
3	−51.32
4	−33.28

[a] Lattice energies for **1** and **2** are given as the average value for the two molecules in the asymmetric unit.

mation (Table 5). As a consequence of the N−H groups being replaced by N−Me units there are no longer any classical hydrogen bond donors. This means that there are a number of weaker interactions involving C−H···O interactions to the carbonyl oxygen. These range from 2.29 to 2.62 Å, as given in Table 7. It is interesting to note that structure **4** has the shortest C−H···O contacts of all the structures described in this study. This reflects the increased importance of these interactions as the classical hydrogen-bonding options decrease.

Lattice Energy Calculations and Intermolecular Interactions. To quantify the contributions of the main interactions the programs HABIT and HABIT 95[19] were used. The lattice energy was calculated using a force-field including hydrogen bonding potentials,[20] the charges from MOPAC/AM1[17,18] and a summation limit of 50 Å. A description of the methods for calculating the lattice energies of molecular materials and their validation has been described elsewhere.[21,22] The lattice energies for structures **1**−**4** are given in Table 8. The values for **1** and **2** were calculated for each of the molecules in the asymmetric unit and averaged.

A comparison of the lattice energies of the four structures shows that the structures with the strongest hydrogen-bonding contributions have the better lattice energies. In a previous paper[12] detailing the structure of **3**, the contribution of various fragments to the overall lattice energy was estimated. On the basis of these data, the predicted reduction in the lattice energy due to the removal of the hydroxyl groups would be 9.73 kcal/mol. This is in good agreement with the difference of 10.43 kcal/mol between the lattice energies of **1** and **3** reported here. Removal of the hydroxyl groups limits the variety of interactions available to the molecule. This accounts for the change between a 3-dimensional network structure in the crystal of **3** and the crystal structure of **1** which is driven by only one strong interaction type. Blockage of the amino donor site in **4** also shows a change in the total lattice energy, as compared to **1**, of 7.61 kcal/mol.

In both structures **1** and **2** the most important interactions are along the stack following the *b*-axis.

Table 9. Breakdown of the Interaction Contributions to the Total Lattice Energy[a]

					total energy (kcal/mol)		
U	*V*	*W*	*Z*	*J*	**1**	**2**	description
0	0	0	1	1	−11.14	−9.79	N2-H···O1′
0	−1	0	3	1	−10.46	−9.55	N1-H···O2

[a] Taken from HABIT based on the atomic coordinates described in the Supporting Information. The central molecule would be *UVW* (0,0,0) and $Z = 1$. Given that there are two molecules in the asymmetric unit, these calculations are centered on molecule 1 (i.e., $J = 1$).

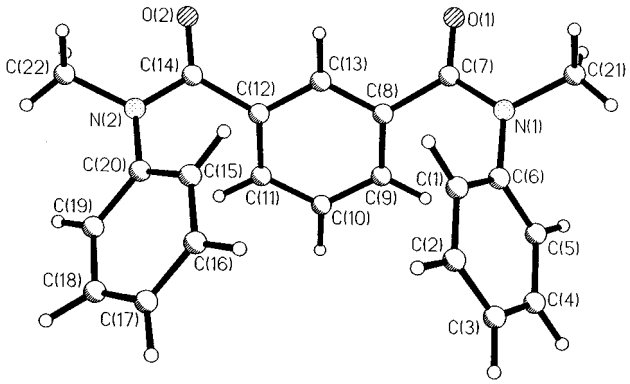

Figure 8. Crystallographic projection of compound **4**.

Table 10. Individual Atom Contributions to the Total Lattice Energy for 1 and 2 (See Figure 3 for Atom Labels of 1 and Figure 4 for Labels of 2)

	percentage contribution	
atom name	**1**	**2**
C7	0.49	2.00
O1	11.16	8.56
N1	3.97	3.28
H(N1)	2.61	2.71
C14	1.06	2.46
O2	9.67	8.13
N2	3.32	2.99
H(N2)	3.37	3.07

These are given in Table 9. The stack for **1** has interaction energies of −11.14 and −10.46 kcal/mol up and down the stack. In **2** the hydrogen bonds are slightly longer and weaker than in **1**, and this is reflected in the lower stacking interactions of −9.79 and −9.55 kcal/mol. The difference in the stacking energy largely accounts for the difference in the lattice energies between **1** and **2** of 2.14 kcal/mol.

The individual contributions of each atom of the amido unit to the total lattice energies for **1** and **2** are given in Table 10. In each of **1**−**3** the percentage contribution to the overall lattice energy, given in Table 11, of the carbonyl groups (i.e., the sum of the C and O atom contributions) is approximately 10%. In **4** this percentage is only 5.15 kcal/mol for one of the carbonyl groups. This can be explained by the fact that the second carbonyl is involved in two C−H···O interactions, whereas the first is involved in only one. The lattice energy contribution for each of the N−CH_3 groups is 7.39% and 10.35%.

The crystal structure of **4** (one molecule of which is shown in Figure 8) can be described as a line of molecules linked by special interactions between H19··· O2 and H18···O1, the geometric details of which are given in Table 7. This is in the direction of the *b*-axis. Along the *c*-axis there is an interaction H4···O2. These

(19) Clydesdale, G.; Docherty R.; Roberts, K. J. *Comput. Phys. Commun.* **1991**, *64*, 311. Clydesdale, G.; Docherty R.; Roberts, K. J. *J. Cryst. Growth* **1996**, *166*, 78. Clydesdale, G.; Docherty R.; Roberts, K. J. *Crystal Growth of Organic Materials*; Myerson, A. S., Green, D. A., Meenan, P., Eds.; American Chemical Society: Washington, DC, 1996; p 43.
(20) Monamy, F. A.; Carruthers, L. M.; McGuire, R. F.; Scheraga, H. A. *J. Phys. Chem.* **1974**, *78*, 1595.
(21) Charlton, M. H.; Docherty R.; Hutchings, M. G. *J. Chem. Soc., Perkin Trans 2* **1995** 2023.
(22) Gavezzotti, A.; Filippini, G. *J. Phys. Chem.* **1994**, *98*, 4831.
(23) Allen, F. H.; Kennard, O. *Chem. Des. Automat. News* **1993**, *8*, 31.
(24) Yang, J.; Fan, E.; Geib S. J.; Hamilton, A. D. *J. Am. Chem. Soc.* **1993**, *115*, 5314.
(25) Geib, S. J.; Vicent, C.; Fan, E.; Hamilton, A. D. *Angew. Chem., Int. Ed. Engl.* **1993**, *32*, 119.
(26) Vyas, K.; Rao V. M.; Manohar, H. *Acta Crystallogr. C* **1987**, *43*, 1201.

Table 11. Contributions of the Named Groups in Each of Structures 1−4

group	1	2	3	4
C═O	10.73	10.59	10.65	9.54
	11.65	10.56	10.78	5.15
N−H	6.69	6.06	3.71	N/A
	6.58	5.99	4.44	N/A
O−H	N/A	N/A	9.70	N/A
	N/A	N/A	9.76	N/A

three hydrogens, H18, H19, and H4, are worth 2.75, 4.69, and 4.26% of the overall lattice energy, respectively, which shows a deviation from the average value for all the aromatic hydrogens of 3.54%. The lines are linked through interactions involving methyl hydrogens and interactions between aromatic hydrogens and aromatic carbons.

Conclusions

In the solid-state *N*,*N*′-diphenylisophthalamide (**1**) and pyridine-2,6-dicarboxylic acid bisphenylamide (**2**) are isostructural. The two pendent amidophenyl units of **1** and **2** both adopt syn−syn confromations. This is in agreement with the calculated heats of formation of the possible conformers. The differences between the syn−syn and other conformers is greater for **2** than for **1** due to the presence of intramolecular hydrogen bonding which, in **2**, produces subtle changes to the syn−syn molecular conformation, making **2** more nearly planar. Consequently the intermolecular hydrogen bonds are lengthened. This is reflected in the lattice energies of −40.89 kcal/mol (**1**) and −38.75 kcal/mol (**2**). Detailed examination of the contributing intermolecular interactions shows that this difference can be attributed to the difference in the stacking energy of 2.3 kcal, with **2** being less stable.

On proceeding from structures **3** to **1** to **4** there is a reduction in the lattice energy. The difference between **3** and **1** is the removal of the OH group. Its contribution was determined in a previous study[12] to be around 9.7 kcal/mol and this is confirmed by the difference in the lattice energies (−10.43 kcal/mol) reported in the present study.

The overall contributions to the lattice energies (in percentage terms) of the C═O units remains consistent across the structures **1**−**3**. In structure **4** they become less important probably due to the lack of "classical" hydrogen-bonding options. The importance of C−H···O interactions in **4** is reflected by the shortest contacts observed for this interaction type in the structures examined. The increasing contribution of certain hydrogen atoms to the overall lattice energy is supportive of the importance of C−H···O intermolecular bonding.

Other structures of this type are currently being synthesized and their structural chemistry will be reported later.

Acknowledgment. C.M.M. wishes to thank D.E.N.I. and Zeneca Specialties for financial support.

Supporting Information Available: Full crystal characterization, atomic coordinates, bond lengths and angles, and anisotropic temperature factors have been deposited as Supporting Information and to the Cambridge Crystallographic Data Centre (10 pages); crystal structure factors (12 pages). Ordering information is given on any current masthead page.

CM970350T